
# Lewis Basicity of Nitrogen-Doped Graphite Observed by CO2 Chemisorption

| | |
|---|---|
| 著者 | Kiuchi Hisao, Shibuya Riku, Kondo Takahiro, Nakamura Junji, Niwa Hideharu, Miyawaki Jun, Kawai Maki, Oshima Masaharu, Harada Yoshihisa |
| journal or publication title | Nanoscale Research Letters |
| volume | 11 |
| number | 1277 |
| year | 2016-03 |
| 権利 | (C) 2016 Kiuchi et al.<br>Open Access This article is distributed under the terms of the Creative Commons Attribution 4.0 International License (http://creativecommons.org/licenses/by/4.0/), which permits unrestricted use, distribution, and reproduction in any medium, provided you give appropriate credit to the original author(s) and the source, provide a link to the Creative Commons license, and indicate if changes were made |
| URL | http://hdl.handle.net/2241/00145331 |

doi: 10.1186/s11671-016-1344-6



Kiuchi et al. Nanoscale Research Letters (2016) 11:127
DOI 10.1186/s11671-016-1344-6

Nanoscale Research Letters
a SpringerOpen Journal

NANO EXPRESS Open Access

# Lewis Basicity of Nitrogen-Doped Graphite Observed by $CO_2$ Chemisorption

Hisao Kiuchi[1], Riku Shibuya[2], Takahiro Kondo[2], Junji Nakamura[2], Hideharu Niwa[3,4,5], Jun Miyawaki[3,4], Maki Kawai[1], Masaharu Oshima[4] and Yoshihisa Harada[3,4*]

## Abstract

The characteristics of $CO_2$ adsorption sites on a nitrogen-doped graphite model system (N-HOPG) were investigated by X-ray photoelectron and absorption spectroscopy and infrared reflection absorption spectroscopy. Adsorbed $CO_2$ was observed lying flat on N-HOPG, stabilized by a charge transfer from the substrate. This demonstrated that Lewis base sites were formed by the incorporation of nitrogen via low-energy nitrogen-ion sputtering. The possible roles of twofold coordinated pyridinic N and threefold coordinated valley N (graphitic N) sites in Lewis base site formation on N-HOPG are discussed. The presence of these nitrogen species focused on the appropriate interaction strength of $CO_2$ indicates the potential to fine-tune the Lewis basicity of carbon-based catalysts.

**Keywords:** $CO_2$ adsorption, Nitrogen-doped carbon, Lewis basicity, X-ray photoelectron spectroscopy, X-ray absorption spectroscopy, Infrared reflection absorption spectroscopy

## Background

The problem of capturing and storing of $CO_2$ as a primary greenhouse gas must be solved to alleviate global warming. Captured $CO_2$ is typically utilized as a simple carbon-containing feedstock (C1) for generating industrially relevant organic molecules [1]. Numerous porous solid adsorbates such as zeolites [2], metal-organic frameworks [3], and mesoporous carbons [4, 5] have been proposed for the effective capture and processing of $CO_2$. Some research groups have reported that nitrogen-doped carbon materials interact more effectively with $CO_2$ than inactive carbon materials do [4–8]. Furthermore, they are also expected as promising electrocatalysts for $CO_2$ and oxygen reduction reaction [8, 9]. Accordingly, the nitrogen doping of carbon materials is expected to be an effective processes to enhance $CO_2$ storage capacity and $CO_2$ reactivity. $CO_2$ is a weak Lewis acid with an electropositive carbon atom that can detect nitrogen-doping-induced basic sites on carbon materials [10, 11]; this detection is classified as a Lewis acid/base reaction.

For practical uses of $CO_2$ adsorbents or catalysts, it is important to balance effective capturing and reduction reaction. A theoretical $CO_2$ adsorption mechanism has been proposed for the catalysts and capturing materials currently in use. For example, hydrogen bonds may form between the surface functional groups and the oxygen atoms of a $CO_2$ molecule [6]; pyridonic nitrogen species may act as anchors for $CO_2$ capture [7]; lone-pair electrons of pyridinic nitrogen may be active for $CO_2$ reduction [8]. However, detailed experimental information regarding the chemical state and geometry of adsorbed $CO_2$ on nitrogen-doped carbon materials is scarce, which hinders the design of effective, highly selective $CO_2$ capturing materials and catalysts for $CO_2$ reduction.

In this study, we investigated the adsorption properties of $CO_2$ on nitrogen-doped graphite (N-HOPG), synthesized using low-energy nitrogen-ion sputtering, using X-ray photoelectron spectroscopy (XPS), angle-resolved X-ray absorption spectroscopy (XAS), and infrared reflection-absorption spectroscopy (IRAS). Using the highly graphitized model N-HOPG with selective nitrogen doping, we discuss the possible contribution of nitrogen components to the formation of Lewis base sites on N-HOPG.

* Correspondence: harada@issp.u-tokyo.ac.jp
[3]The Institute for Solid State Physics (ISSP), the University of Tokyo, Kashiwa, Chiba, Japan
[4]Synchrotron Radiation Research Organization, the University of Tokyo, Kashiwa, Chiba, Japan
Full list of author information is available at the end of the article

## Methods

A cleaved highly oriented pyrolytic graphite (HOPG, PGCSTM, Panasonic Inc.) plate was annealed at 1000 K for 30 min in an ultra-high vacuum (UHV) ($<5 \times 10^{-7}$ Pa), sputtered with $8 \times 10^{13}$ nitrogen ions $cm^{-2}$ at 200 eV (equivalent to 2 % nitrogen relative to the surface carbon atoms) at 300 K using an ion gun (OMI-0730, Omegatron Inc.), and annealed again at 1000 K for 1 h for surface cleaning [12].

XPS measurements were performed at BL27SU in a third-generation synchrotron radiation facility SPring-8 using a photoelectron analyzer (PHOIBOS 150, SPECS). The typical base pressures for the measurement and preparation chambers were $4 \times 10^{-8}$ and $3 \times 10^{-7}$ Pa, respectively. The incident photon energy and the photoemission angle were 850 eV and 45°, respectively. The total energy resolution of the XPS was 230 meV. Samples were scanned with the incident photon beam at a rate of 0.4 μm $s^{-1}$ to reduce the radiation damage to the adsorbed molecules. The binding energies were calibrated using the Au $4f_{7/2}$ (binding energy = 84.0 eV) peak of an evaporated gold as a reference. The N 1*s* spectra were fitted with the Voigt function (1.2 and 0.25 eV Gaussian and Lorentzian widths, respectively) as well as background subtraction using the Shirley method. The normalized intensity of each peak was calculated by multiplying the integrated intensity and the cross section of each element. N/C and O/C ratios were calculated by dividing the normalized intensities of the N 1*s* and O 1*s* spectra by that of C 1*s* spectrum, respectively. The surface nitrogen density was estimated by an assumption that nitrogen atoms are located only at the first graphite layer of HOPG. When we take into account the attenuation of photoelectrons in the bulk region, the contribution to the photoelectron from the first layer is calculated by $1-\exp(-d/\lambda\cos\theta)$ where $d$ is the interlayer distance, $\lambda$ is the inelastic mean free path, and $\theta$ is the photoemission angle. In the present case for the C 1*s* XPS spectrum of graphite, this value is estimated to be 0.33 where $d$ is 3.354 Å, $\lambda$ is 11.77 Å [13] at 561 eV of kinetic energy which is obtained by subtracting the core level of C 1*s* (~284 eV) and work function of graphite (4.6 eV) [14] from the incident photon energy $h\nu$ = 850 eV, and $\theta$ is 45°. Therefore, the surface nitrogen and the adsorbed $CO_2$ densities (ML) are estimated by dividing the normalized intensities of the N 1*s* and O 1*s* XPS spectra by one third of that of the C 1*s* spectrum, respectively. Here, the number of the 1 ML nitrogen atoms is defined as that of the carbon atoms at the first graphite layer ($3.82 \times 10^{15}$ atoms $cm^{-2}$). The number of the adsorbed 1 ML $CO_2$ molecules is also defined as that of the carbon atoms at the first graphite layer and to get the number of $CO_2$ molecules, the estimated value from O 1*s* XPS should be divided by 2 since $CO_2$ is composed of two oxygen atoms and one carbon atom.

N 1*s* and O 1*s* XAS spectra were measured by the partial electron yield (PEY) mode at BL27SU. The XAS spectra were collected by setting the angle $\theta$ between the incident X-ray beam axis and the surface normal to 0°, 45°, and 70°. The energy resolution of XAS had a lower limit below 100 meV.

The N-HOPG was annealed at 1000 K for 30 min in the preparation chamber to remove the initially adsorbed gas before the XPS and XAS measurements were performed. The sample was exposed to $CO_2$ at 300 K for 2500 s at $5.3 \times 10^{-4}$ Pa, corresponding to 10,000 L in volume.

IRAS measurements were performed in grazing-angle reflection geometry both before and after $CO_2$ adsorption at 300 K to investigate the configuration of the adsorbed $CO_2$. In order to estimate the amount of the adsorbed $CO_2$, temperature-programmed desorption (TPD) was performed between 300 and 700 K, with $CO_2$ adsorption at 300 K. Both the IRAS and TPD experiments were performed in the same UHV ($3 \times 10^{-8}$ Pa) chamber.

## Results and Discussion

Figure 1a shows the C 1*s* XPS spectra of HOPG and N-HOPG. The spectral intensities are normalized to the peak areas. The nitrogen ion sputtering causes the C 1*s* peak to broaden and introduces the C=N bond peak at 285.6 eV [15]. Figure 1b shows the N 1*s* XPS spectrum of N-HOPG. The N/C ratio and surface nitrogen density are calculated to be 0.0042 and 0.013 ML, respectively. The spectrum is fitted with four Voigt functions corresponding to each nitrogen component, denoted as pyridinic N (398.0 eV), cyanide N (399.9 eV), center N (401.0 eV), and valley N (401.9 eV). The terminology of the nitrogen components used hereafter is represented in Fig. 1c. Pyridinic N is connected to two carbon atoms and exists either at graphite edges or in the basal plane of graphite with a monovacancy [16]. Cyanide N has triple bonds between the nitrogen and carbon atoms [17]. Both center N and valley N are graphitic N connected to three carbon atoms, existing in the graphite basal plane, and at graphite zigzag edges or vacancy sites, respectively [18, 19]. The detailed peak assignment of each component was discussed in our previous report [12]. The estimated amount of each nitrogen component from the fitting results is summarized in Table 1; center N is the most prevalent, followed by valley N and pyridinic N.

Figure 2a shows the estimated area intensity of the mass 44 ($CO_2$) peak as a function of $CO_2$ exposure obtained by the TPD measurements. The saturation amount of adsorbed $CO_2$ on N-HOPG is near 10,000 L;

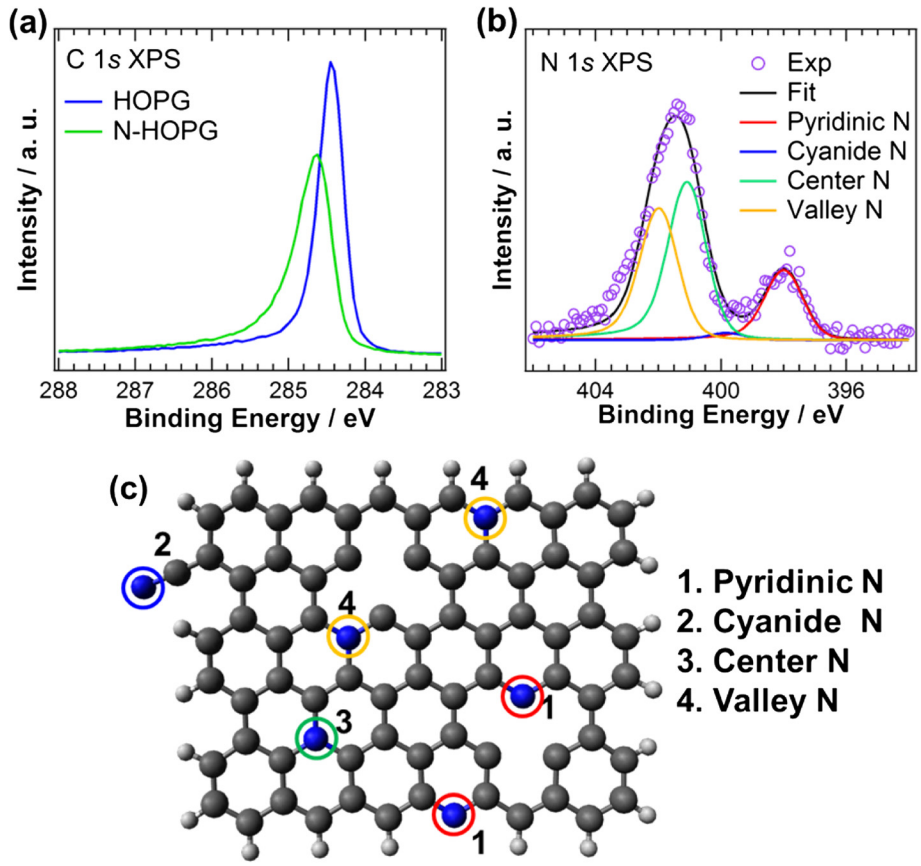


**Fig. 1** XPS spectra of HOPG and N-HOPG before $CO_2$ adsorption. **a** C 1*s* XPS. **b** N 1*s* XPS. **c** A schematic of each nitrogen configuration in N-HOPG. Hydrogen, carbon, and nitrogen atoms are represented by *white*, *black*, and *blue balls*, respectively

this amount was used for the XPS and XAS measurements. A clear $CO_2$ desorption peak is observed between 320 and 400 K, which approaches the temperature of $CO_2$ desorption for nitrogen-doped graphite model catalysts [20]. In addition, the amount of the adsorbed $CO_2$ on N-HOPG is almost constant when 5000 L $CO_2$ exposure was performed twice as shown in Fig. 2a, which indicates $CO_2$ adsorption is reversible without poisoning. In contrast, only physisorbed $CO_2$ was reported on HOPG, which desorbed at 83 K with the desorption energy of 20 kJ $mol^{-1}$ [21]. Therefore, nitrogen doping forms $CO_2$ adsorption sites at 300 K on the HOPG surface. Figure 2b, c shows O 1*s* XPS spectra of HOPG and N-HOPG before and after $CO_2$ adsorption, respectively. A very small amount of oxygen species (O/C = 0.04 at.%) exists in N-HOPG before $CO_2$ adsorption, as shown in Fig. 2c, which are not fully removed by annealing at 1000 K for 30 min. The difference spectrum in Fig. 2c shows an O 1*s* peak centered at approximately 533 eV caused by $CO_2$ adsorption on N-HOPG. The extracted O/C ratio and the adsorbed $CO_2$ density are calculated to be 0.00023 and 0.00035 ML, respectively, based on the procedure described in the "Methods" section. However, the difference spectrum in Fig. 2b of HOPG shows no peak related to adsorbed $CO_2$. Table 2 summarizes the O 1*s* binding energies for physisorbed and chemisorbed $CO_2$ on various substrates [22–27]; for physisorbed $CO_2$, the binding energy is distributed from 534.0 to 535.8 eV, while for chemisorbed $CO_2$, it ranges from 530.6 to 533 eV. The observed $CO_2$ binding energy at 533 eV on N-HOPG is below that of physisorbed $CO_2$ but within the range of chemisorption. The interaction strength of $CO_2$ directly estimates the degree of Lewis basicity of the N-HOPG substrate. To determine the origin of this binding energy, we discuss the electronic structure of $CO_2$ as presented by a Walsh diagram in Fig. 2d [28]. The lowest unoccupied molecular orbital (LUMO) of $2\pi_u$ is degenerated in the linear configuration, while it splits into $2b_1$ (perpendicular to the $CO_2$

**Table 1** Surface nitrogen density and relative ratio of each nitrogen component

| Type of nitrogen | Pyridinic N | Cyanide N | Center N | Valley N |
|---|---|---|---|---|
| Nitrogen density/ML | 0.0024 | 0.0002 | 0.0054 | 0.0045 |
| Relative ratio/% | 19 | 2 | 43 | 36 |

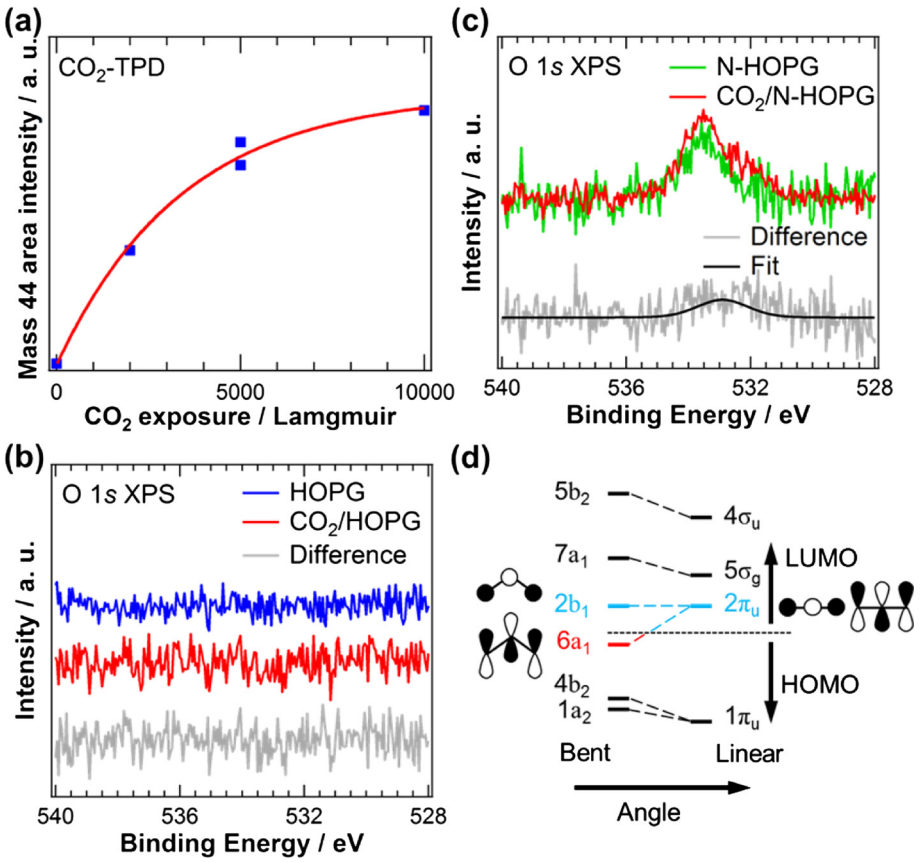


**Fig. 2** **a** The area intensity of the mass 44 ($CO_2$) peak as a function of the $CO_2$ exposure. O 1*s* XPS spectra of **b** HOPG and **c** N-HOPG before and after $CO_2$ adsorption. **d** A schematic of the Walsh diagram of $CO_2$ orbital energies in linear and bent geometries

plane) and $6a_1$ (parallel to the $CO_2$ plane) orbitals in the bent configuration. In particular, the energy position of $6a_1$ orbital sharply decreases upon bending. In the bent configuration, this low-energy $6a_1$ orbital is occupied by electrons charge-transferred from the substrate and stabilizes the adsorbed $CO_2$ molecules on N-HOPG. Thus, the charge transfer from the substrate to the $6a_1$ orbital in the bent configuration weakens the strength of CO bonds, causing the O 1*s* core level shift of $CO_2$ to the lower binding energy at approximately 533 eV. This result also provides evidence for the presence of Lewis base sites in the graphite system caused by the doped nitrogen.

In order to reveal the orientation of the adsorbed $CO_2$ on N-HOPG, angle-resolved XAS was performed. Figure 3a shows the O 1*s* XAS spectra of N-HOPG after $CO_2$ adsorption for different incident angles $\theta$, where the background XAS profile obtained before $CO_2$

**Table 2** O 1*s* binding energies for physisorbed and chemisorbed $CO_2$ on various substrates

| Substrate | O 1*s* binding energy/eV | | Ref. |
|---|---|---|---|
| | Physisorption ($CO_2$) | Chemisorption ($CO_2^{\delta-}$) | |
| Ni(110) | 534.7 | 531.1 | [22] |
| Ni(110) | 534 | 530.6 | [23] |
| Fe(poly) | 535 | 531 | [22] |
| $Cr_2O_3$(0001) | – | 532.5 | [24, 25] |
| K doped Rh(111) | 534.7 | 532.8 | [26] |
| K doped $Mo_2C$ | 535.8 | 533 | [27] |
| N doped HOPG | – | 533 | This work |

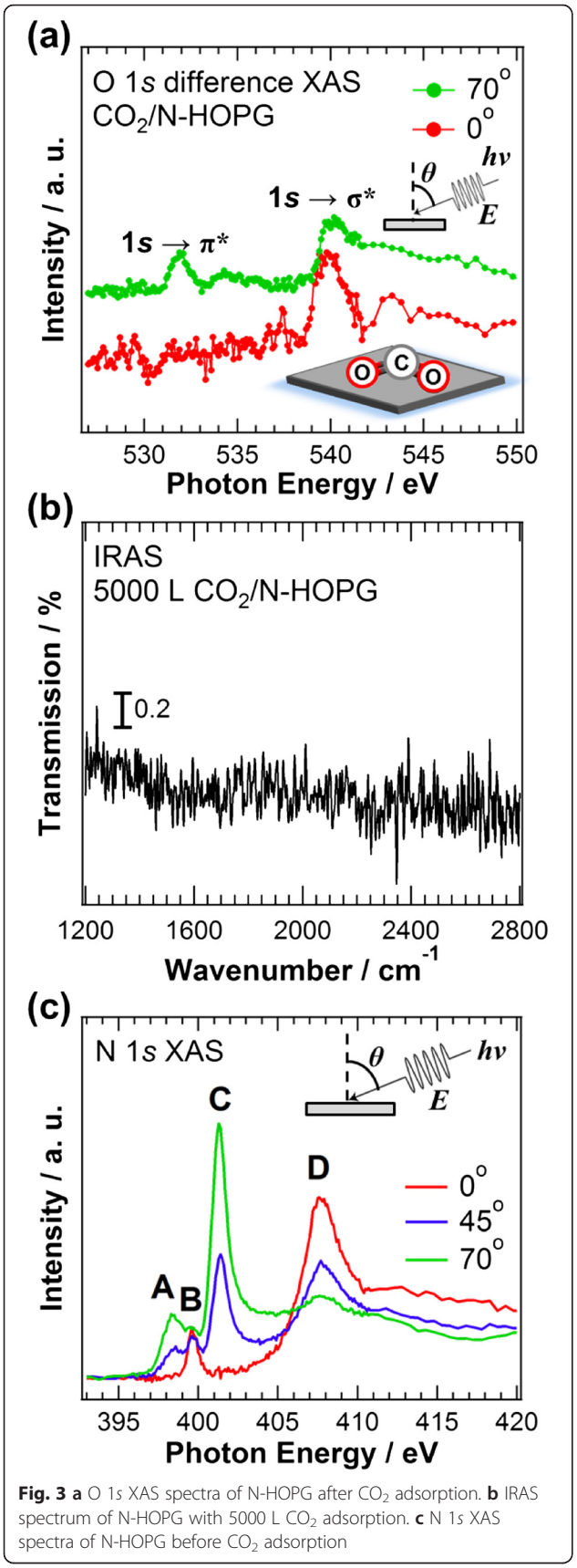


**Fig. 3** **a** O 1*s* XAS spectra of N-HOPG after $CO_2$ adsorption. **b** IRAS spectrum of N-HOPG with 5000 L $CO_2$ adsorption. **c** N 1*s* XAS spectra of N-HOPG before $CO_2$ adsorption

adsorption is subtracted. The σ* (540 eV) and π* (532 eV) peaks are enhanced at surface normal (0°) and grazing (70°) incidence, respectively. The observed π* orbital would be derived from the $2b_1$ orbital (perpendicular to the $CO_2$ plane) caused by the splitting of $CO_2$ LUMO orbitals. Therefore, this polarization dependence of O 1*s* XAS indicates that the $CO_2$ molecules are lying flat on the N-HOPG surface. Although the energy position of the $6a_1$ orbital sharply decreases upon bending, the energy position of the $2b_1$ orbital remains nearly constant relative to that of the $2\pi_u$ orbital, as shown in Fig. 2d. The observed π* peak is ~2.8 eV lower than the π* peak ($2\pi_u$ orbital) for the gas-phase linear $CO_2$ at 534.8 eV [29], mainly because of the observed chemical shift of the O 1*s* core level in XPS, as discussed above.

The IRAS spectrum in Fig. 3b also supports the above $CO_2$ configuration; considering the selection rule of IRAS, the absence of peaks at approximately 1200–1300 $cm^{-1}$ and 1600 $cm^{-1}$, expected for the symmetric and asymmetric OCO-stretching modes of the bent $CO_2^{\delta-}$ carboxylate with its molecular plane perpendicular to the surface [25], suggests the $CO_2$ to be lying flat on the surface. Both the O 1*s* XAS spectra and the IRAS spectrum of the N-HOPG support this configuration of the adsorbed $CO_2$.

Figure 3c shows the N 1*s* XAS spectra of the N-HOPG before $CO_2$ adsorption for different incident angles of 0°, 45°, and 70°. The spectra are normalized according to the intensity at 430 eV. Three sharp peaks in the π* region can be assigned to pyridinic N (A), cyanide N (B), and graphitic N (center N and valley N) (C) [12, 30]. A peak at 407.5 eV corresponds to the σ* state of the nitrogen components. The intensities of the pyridinic and graphitic N change with the X-ray incident angles, indicating that these components are incorporated into the planar graphite lattice via substitution [31]. The cyanide N, however, does not show any polarization dependence, suggesting multiple directions of the C≡N configuration. Since the adsorbed $CO_2$ also shows a highly oriented (lying flat) configuration, $CO_2$ adsorption sites should be introduced in the vicinity of the highly oriented pyridinic and graphitic N (center N and valley N).

Based on the Lewis acid/base-interaction picture, several research groups have reported possible mechanisms of $CO_2$ adsorption and reduction on nitrogen-doped carbon materials as follows: (1) hydrogen bonds forming between the carbon surface and oxygen atoms in a $CO_2$ molecule [6], (2) pyridonic N species as anchors for $CO_2$ capture [7], (3) a lone-pair electron located at a nitrogen atom [8], and (4) a localized electronic state of the graphite surface modified by doped nitrogen [20, 32–34]. The possibility of mechanism (1) can be excluded, because hydrogen atoms are much less prevalent in the large

platelet graphite used in this study than they can be in graphene flakes. Mechanism (2) can also be excluded because pyridonic N species, located at approximately 400 eV [7], are not observed in the N 1*s* XPS spectrum. For the presence of a lone-pair electron that interacts with $CO_2$, the most probable amine functional groups, located at 399.4 eV [16], are not observed because of the pyrolysis at ~1000 K in this work, but pyridinic N, which is present in this work, provides a possibility for mechanism (3) [8]. We consider that mechanism (4) is the most probable for creating the active sites for $CO_2$ adsorption and reduction. The pyridinic N detected in our results may work as a Lewis base and interact with $CO_2$. Indeed, recent scanning tunneling spectroscopy measurements have revealed the presence of an electronic structure just 370 meV below the Fermi level of several localized carbon atoms surrounding pyridinic N at monovacancy sites [33]. The observed valley N site is also expected to modify the electronic structure of the surrounding carbon atoms and induce a local density of states of ~200–400 meV below the Fermi level [34], which may also provide $CO_2$ adsorption and reaction sites. Therefore, the interaction sites with $CO_2$ in N-HOPG would be provided by the lone-pair electrons of pyridinic N or the localized π states just below the Fermi level induced by the pyridinic N and/or valley N. According to the recent report with HOPG model catalysts, pyridinic N can create Lewis base sites for $CO_2$ adsorption on carbon materials [20], which is consistent with our present discussion. The clear evidence of the charge transfer from the substrate and the new information on the molecular orientations of both $CO_2$ and nitrogen moieties on the graphite substrate provide great insight into the $CO_2$ adsorption mechanism, and the Lewis basicity of nitrogen-doped graphite can be directly estimated by element-specific synchrotron analyses.

## Conclusions

We have investigated the adsorbed $CO_2$ at 300 K on N-HOPG by XPS, angle-resolved XAS, and IRAS using a model N-HOPG synthesized by a protocol developed in a previous study. The O 1*s* binding energy of the adsorbed $CO_2$ at 300 K, located at 533 eV, showed clear evidence of the Lewis basicity of N-HOPG caused by the nitrogen doped in the graphite system. The polarization dependence of the σ* and π* peaks in the O 1*s* XAS spectra, as well as the absence of expected IRAS signals, clearly indicates that the adsorbed $CO_2$ lies flat on the graphite surface and that Lewis base sites are induced by the incorporation of nitrogen in HOPG. We discussed possible $CO_2$ adsorption sites induced by pyridinic N and valley N species. The activity of these species as adsorption sites indicates the potential to fine-tune the Lewis basicity of a graphite substrate by controlling the prevalence of nitrogen species focused on the appropriate interaction strength of $CO_2$, which can be directly estimated by the O 1*s* binding energy of the adsorbed $CO_2$. The properties of fine-tuned Lewis basicity in carbon-based materials can be applied to the field of catalysis, including the use of the materials as oxygen reduction reaction or hydrogen evolution reaction sites.

#### Abbreviations

$CO_2$: carbon dioxide; HOPG: highly oriented pyrolytic graphite; IRAS: infrared reflection-absorption spectroscopy; LUMO: lowest unoccupied molecular orbital; N-HOPG: nitrogen doped highly oriented pyrolytic graphite; PEY: partial electron yield; TPD: temperature-programmed desorption; UHV: ultra-high vacuum; XAS: X-ray absorption spectroscopy; XPS: X-ray photoelectron spectroscopy.

#### Competing Interests

The authors declare that they have no competing interests.

#### Authors' Contributions

HK carried out all the experiments, prepared the N-HOPG, and drafted the manuscript. RS and TK carried out all the experiments and discussion of the study. HN and JM carried out the XPS and XAS measurements, participated in the discussion of the study, and helped to draft the manuscript. YH participated in the coordination and discussion of the study and helped in drafting the manuscript. JN, MK, and MO participated in the design and coordination of the study and helped to revise the manuscript. All authors read and approved the final manuscript.

#### Acknowledgements

This work was financially supported by the New Energy and Industrial Technology Development Organization (NEDO), Japan. The authors thank T. Muro for their technical support in the BL27SU experiments in SPring-8 (Proposal Nos. 2014A1390, 2014B1526, and 2015A1591). XAS experiments at BL07LSU in SPring-8 were performed jointly in the Synchrotron Radiation Research Organization and Institute for Solid State Physics, at the University of Tokyo, Japan (Proposal Nos. 2013B7403 and 2014B7403). Preliminary experiments at KEK-PF were performed under the approval of the Photon Factory Program Advisory Committee (Proposal No. 2010G669). HK acknowledges support from Japan Society for the Promotion of Science (JSPS) Research Fellowship for Young Scientists and the JSPS Program for Leading Graduate Schools (MERIT). TK appreciates the financial support by the PRESTO (Precursory Research for Embryonic Science and Technology) program in The Japan Science and Technology Agency (JST), "New Materials Science and Element Strategy".

#### Author details

[1]Department of Applied Chemistry, the University of Tokyo, 7-3-1 Hongo, Bunkyo-ku, Tokyo 113-8656, Japan. [2]Faculty of Pure and Applied Sciences, University of Tsukuba, Ibaraki, Japan. [3]The Institute for Solid State Physics (ISSP), the University of Tokyo, Kashiwa, Chiba, Japan. [4]Synchrotron Radiation Research Organization, the University of Tokyo, Kashiwa, Chiba, Japan. [5]Present address: Graduate School of Pure and Applied Sciences, University of Tsukuba, Ibaraki, Japan.

Received: 19 January 2016 Accepted: 27 February 2016
Published online: 08 March 2016

#### References

1. Arakawa H, Aresta M, Armor JN, Barteau MA, Beckman EJ, Bell AT et al (2001) Catalysis research of relevance to carbon management: progress, challenges, and opportunities. Chem Rev 101:953–96
2. Choi S, Drese JH, Jones CW (2009) Adsorbent materials for carbon dioxide capture from large anthropogenic point sources. ChemSusChem 2:796–854
3. McDonald TM, Mason JA, Kong X, Bloch ED, Gygi D, Dani A et al (2015) Cooperative insertion of $CO_2$ in diamine-appended metal-organic frameworks. Nature 519:303–8
4. Wang Y, Zou H, Zeng S, Pan Y, Wang R, Wang X et al (2015) A one-step carbonization route towards nitrogen-doped porous carbon hollow spheres

with ultrahigh nitrogen content for $CO_2$ adsorption. Chem Commun 51: 12423–6
5. Wei J, Zhou D, Sun Z, Deng Y, Xia Y, Zhao D (2013) A controllable synthesis of rich nitrogen-doped ordered mesoporous carbon for $CO_2$ capture and supercapacitors. Adv Funct Mater 23:2322–8
6. Xing W, Liu C, Zhou Z, Zhang L, Zhou J, Zhuo S et al (2012) Superior $CO_2$ uptake of N-doped activated carbon through hydrogen-bonding interaction. Energy Environ Sci 5:7323–7
7. Sevilla M, Valle-Vigón P, Fuertes AB (2011) N-doped polypyrrole-based porous carbons for $CO_2$ capture. Adv Funct Mater 21:2781–7
8. Sharma PP, Wu J, Yadav RM, Liu M, Wright CJ, Tiwary CS et al (2015) Nitrogen-doped carbon nanotube arrays for high-efficiency electrochemical reduction of CO2: on the understanding of defects, defect density, and selectivity. Angew Chemie Int Ed 54:13701–5
9. Gong K, Du F, Xia Z, Durstock M, Dai L (2009) Nitrogen-doped carbon nanotube arrays with high electrocatalytic activity for oxygen reduction. Science 323:760–4
10. Auroux A, Gervasini A (1990) Microcalorimetric study of the acidity and basicity of metal oxide surfaces. J Phys Chem 94:6371–9
11. Lavalley JC (1996) Infrared spectrometric studies of the surface basicity of metal oxides and zeolites using adsorbed probe molecules. Catal Today 27: 377–401
12. Kiuchi H, Kondo T, Sakurai M, Guo D, Nakamura J, Niwa H et al (2016) Characterization of nitrogen species incorporated into graphite using low energy nitrogen ion sputtering. Phys Chem Chem Phys 18:458–65
13. Tanuma S, Powell CJ, Penn DR (2010) Calculations of electron inelastic mean free paths. IX. Data for 41 elemental solids over the 50 eV to 30 keV range. Surf Interface Anal 43:689–713
14. Takahashi T, Tokailin H, Sagawa T (1985) Angle-resolved ultraviolet photoemission spectroscopy of the unoccupied band structure of graphite. Phys Rev B 32:8317–24
15. Scardamaglia M, Amati M, Llorente B, Mudimela P, Colomer J-F, Ghijsen J et al (2014) Nitrogen ion casting on vertically aligned carbon nanotubes: tip and sidewall chemical modification. Carbon 77:319–28
16. Pels J, Kapteijn F, Moulijn J, Zhu Q, Thomas K (1995) Evolution of nitrogen functionalities in carbonaceous materials during pyrolysis. Carbon 33:1641–53
17. Jansen R, Van Bekkum H (1995) XPS of nitrogen-containing functional groups on activated carbon. Carbon 33:1021
18. Sharifi T, Hu G, Jia X, Wågberg T (2012) Formation of active sites for oxygen reduction reactions by transformation of nitrogen functionalities in nitrogen-doped carbon nanotubes. ACS Nano 6:8904–12
19. Casanovas J, Ricart JM, Rubio J, Illas F, Jiménez-Mateos JM (1996) Origin of the large N 1s binding energy in X-ray photoelectron spectra of calcined carbonaceous materials. J Am Chem Soc 118:8071–6
20. Guo D, Shibuya R, Akiba C, Saji S, Kondo T, Nakamura J. Active sites of nitrogen-doped carbon materials for oxygen reduction reaction clarified using model catalysts. Science. in press.
21. Edridge JL, Freimann K, Burke DJ, Brown WA (2013) Surface science investigations of the role of $CO_2$ in astrophysical ices. Philos Trans R Soc A Math Phys Eng Sci 371:20110578
22. Illing G, Heskett D, Plummer EW, Freund H-J, Somers J, Lindner T et al (1988) Adsorption and reaction of $CO_2$ on Ni{110}: X-ray photoemission, near-edge X-ray absorption fine-structure and diffuse leed studies. Surf Sci 206:1–19
23. Ding X, De Rogatis L, Vesselli E, Baraldi A, Comelli G, Rosei R et al (2007) Interaction of carbon dioxide with Ni(110): a combined experimental and theoretical study. Phys Rev B 76:195425
24. Kuhlenbeck H, Xu C, Dillmann B, Haßel M, Adam B, Ehrlich D et al (1992) Adsorption and reaction on oxide surfaces: CO and $CO_2$ on $Cr_2O_3$(111). Berichte Der Bunsengesellschaft Für Phys Chemie 96:15–27
25. Seiferth O, Wolter K, Dillmann B, Klivenyi G, Freund HJ, Scarano D et al (1999) IR investigations of $CO_2$ adsorption on chromia surfaces: $Cr_2O_3$ (0001)/Cr(110) versus polycrystalline α-$Cr_2O_3$. Surf Sci 421:176–90
26. Kiss J, Révész K, Solymosi F (1988) Photoelectron spectroscop1c studies of the adsorption of $CO_2$ on potassium-promoted Rh(111) surface. Surf Sci 207: 36–54
27. Bugyi L, Oszkó A, Solymosi F (2000) Spectroscopic study on the formation of $CO_2^-$ on K-promoted $Mo_2C$/Mo(100) surface. Surf Sci 461:177–90
28. Freund HJ, Roberts MW (1996) Surface chemistry of carbon dioxide. Surf Sci Rep 25:225–73
29. Maganas D, Kristiansen P, Duda L-C, Knop-Gericke A, DeBeer S, Schlögl R et al (2014) Combined experimental and ab initio multireference configuration interaction study of the resonant inelastic X-ray scattering spectrum of $CO_2$. J Phys Chem C 118:20163–75
30. Schiros T, Nordlund D, Pálová L, Prezzi D, Zhao L, Kim KS et al (2012) Connecting dopant bond type with electronic structure in N-doped graphene. Nano Lett 12:4025–31
31. Shimoyama I, Wu G, Sekiguchi T, Baba Y (2000) Evidence for the existence of nitrogen-substituted graphite structure by polarization dependence of near-edge x-ray-absorption fine structure. Phys Rev B 62:R6053–6
32. Kondo T, Honma Y, Oh J, Machida T, Nakamura J (2010) Edge states propagating from a defect of graphite: scanning tunneling spectroscopy measurements. Phys Rev B 82:153414
33. Kondo T, Casolo S, Suzuki T, Shikano T, Sakurai M, Harada Y et al (2012) Atomic-scale characterization of nitrogen-doped graphite: effects of dopant nitrogen on the local electronic structure of the surrounding carbon atoms. Phys Rev B 86:035436
34. Huang SF, Terakura K, Ozaki T, Ikeda T, Boero M, Oshima M et al (2009) First-principles calculation of the electronic properties of graphene clusters doped with nitrogen and boron: analysis of catalytic activity for the oxygen reduction reaction. Phys Rev B 80:235410